

OPEN

# Relationship Between <sup>18</sup>F-Fluorodeoxyglucose Uptake and V-Ki-Ras2 Kirsten Rat Sarcoma Viral Oncogene Homolog Mutation in Colorectal Cancer Patients

## Variability Depending on C-Reactive Protein Level

Jae-Hoon Lee, MD, Jeonghyun Kang, MD, Seung Hyuk Baik, MD, PhD, Kang Young Lee, MD, PhD, Beom Jin Lim, MD, PhD, Tae Joo Jeon, MD, PhD, Young Hoon Ryu, MD, PhD, and Seung-Kook Sohn, MD, PhD

**Abstract:** To evaluate clinical values of clinicopathologic and <sup>18</sup>F-fluorodeoxyglucose (<sup>18</sup>F-FDG) positron emission tomography/computed tomography (PET/CT)-related parameters for prediction of v-Ki-ras2 Kirsten rat sarcoma viral oncogene homolog (KRAS) mutation in colorectal cancer (CRC) and to investigate their variability depending on C-reactive protein (CRP) levels.

In total, 179 CRC patients who underwent PET/CT scans before curative resection and KRAS mutation evaluation following surgery were enrolled. Maximum standardized uptake value (SUV<sub>max</sub>), peak standardized uptake value (SUV<sub>peak</sub>), metabolic tumor volume, and total lesion glycolysis were determined semiquantitatively. Associations between clinicopathologic and PET/CT-related parameters and KRAS expression were analyzed.

Elevated CRP (>6.0 mg/L; n = 47) was associated with higher primary tumor size, higher SUV<sub>max</sub>, SUV<sub>peak</sub>, metabolic tumor volume, and total lesion glycolysis, compared with those for the group with a CRP lower than that the cutoff value (<6.0 mg/L; n = 132). Interestingly, the CRC patients (having CRP < 6.0 mg/L) with KRAS mutations had significantly higher (*P* < 0.05) SUV<sub>max</sub> and SUV<sub>peak</sub> values than the patients expressing wild-type KRAS mutations. Multivariate analysis revealed SUV<sub>max</sub> and SUV<sub>peak</sub> to be significantly associated with KRAS mutations (odds ratio = 3.3, *P* = 0.005, and odds ratio = 3.9, *P* = 0.004), together with histologic grade and lymph node metastasis.

<sup>18</sup>F-FDG uptake was significantly higher in CRC patients with KRAS mutations and with normal CRP levels. A severe local inflammation with raised CRP levels, however, might affect accurate <sup>18</sup>F-FDG quantification in CRC tumors. Positron emission tomography/computed tomography-related parameters could supplement

genomic analysis to determine KRAS expression in CRC; however, care should be exercised to guarantee proper patient selection.

(*Medicine* 95(1):e2236)

**Abbreviations:** <sup>18</sup>F-FDG = <sup>18</sup>F-fluorodeoxyglucose, BMI = body mass index, CEA = carcinoembryonic antigen, CI = confidence interval, CRC = colorectal cancer, CRP = C-reactive protein, EGFR = epidermal growth factor receptor, GLUT1 = glucose transporter-1, HNPCC = hereditary nonpolyposis colorectal cancer, KRAS = v-Ki-ras2 Kirsten rat sarcoma viral oncogene homolog, LN lymph node, LVI = lymphovascular invasion, MTV = metabolic tumor volume, OR = odds ratio, PET/CT = positron emission tomography/computed tomography, ROC = receiver operating characteristic, SUV<sub>max</sub> = maximum standardized uptake value, SUV<sub>peak</sub> = peak standardized uptake value, TAM = tumor-associated macrophage, TLG = total lesion glycolysis, VEGF = vascular endothelial growth factor, VOI = volume of interest.

## INTRODUCTION

Colorectal cancer (CRC) is the third most common cancer in the world. After curative resection, adjuvant cytotoxic chemotherapy and/or radiotherapy is recommended to improve survival, especially in patients with stage II and III cancer. Although CRC patients presenting with metastatic disease have poor prognosis; nevertheless, some survival benefits are indicated with newer targeted therapies: these therapies include monoclonal antibodies against epidermal growth factor receptor (EGFR) or vascular endothelial growth factor receptors. An augmentation of cetuximab, an EGFR inhibitor, in first line treatment has been reported to reduce the risk of progression in patients with unresectable metastatic CRC disease with v-Ki-ras2 Kirsten rat sarcoma viral oncogene homolog (KRAS) wild-type tumors.<sup>1</sup> Notwithstanding, an accurate identification of patients likely to respond to such targeted therapies may prevent nonresponders from undergoing unwanted drug toxicity and treatment cost.<sup>2</sup> V-Ki-ras2 Kirsten rat sarcoma viral oncogene homolog mutational status as evaluated by histologic tumor examination is detected in approximately 30% to 40% of CRC patients.<sup>3</sup>

<sup>18</sup>F-fluorodeoxyglucose (<sup>18</sup>F-FDG) positron emission tomography/computed tomography (PET/CT) is widely used in various malignancies for diagnosis, treatment response assessment, surveillance, and prognostication.<sup>4</sup> Although preoperative imaging is important for making critical decisions for treatment planning, only a few studies have described relationships between scan findings and KRAS mutation in CRC

Editor: Lalit Banswal.

Received: July 30, 2015; revised: November 11, 2015; accepted: November 12, 2015.

From the Department of Nuclear Medicine (JHL, TJJ, YHR); Department of Surgery (JK, SHB, SKS); Department of Pathology (BJL), Gangnam Severance Hospital, Yonsei University College of Medicine, and Department of Surgery (KYL), Yonsei University College of Medicine, Seoul, South Korea.

Correspondence: Jeonghyun Kang, MD, Department of Surgery, Yonsei University College of Medicine, Gangnam Severance Hospital, 211 Eonju-Ro, Gangnam-Gu, Seoul 06273, South Korea (e-mail: ravic@naver.com).

The authors have no funding and conflicts of interest to disclose.

Copyright © 2016 Wolters Kluwer Health, Inc. All rights reserved.

This is an open access article distributed under the terms of the Creative Commons Attribution-NonCommercial-ShareAlike 4.0 License, which allows others to remix, tweak, and build upon the work non-commercially, as long as the author is credited and the new creations are licensed under the identical terms.

ISSN: 0025-7974

DOI: 10.1097/MD.0000000000002236

patients. Moreover, these studies report conflicting results: 2 clinical studies demonstrated that higher  $^{18}\text{F}$ -FDG uptake in CRC is associated with KRAS mutation,<sup>5,6</sup> and a recent study by Iwamoto et al<sup>7</sup> suggested that upregulation of glucose transporter-1 (GLUT1) is a possible mechanism of higher  $^{18}\text{F}$ -FDG accumulation in CRC with KRAS mutation. Meanwhile, Krikelis et al<sup>8</sup> reported that there is a lack of any association between KRAS mutation and  $^{18}\text{F}$ -FDG-PET scan findings. Although sample size and ethnic differences might be sources of bias, the reasons for this discordance are not clearly understood.

Interestingly, Kawada et al<sup>6</sup> excluded CRC patients who had severe inflammation with C-reactive protein (CRP) levels  $>5.0$  mg/L. CRP is an annular, metamereric protein found in the blood plasma. CRP levels rise in response to inflammation, because CRP is an acute-phase protein of hepatic origin that increases following interleukin-6 secretion from macrophages and T cells. Local inflammation of cancer cells could impact FDG uptake,<sup>9,10</sup> and elevation in CRP may cause false-positive results on  $^{18}\text{F}$ -FDG PET examinations.<sup>11</sup> Although the actual impact of CRP levels on  $^{18}\text{F}$ -FDG uptake in tumors is still unclear, we assumed that abnormal CRP levels might imply the presence of severe inflammation and act as a confounding factor in the association between  $^{18}\text{F}$ -FDG uptake in CRC and KRAS mutation.

In this study, we investigated clinicopathologic variables and PET/CT-related parameters that could potentially predict KRAS mutation in a large population of CRC patients and evaluated the variability of their predictive values according to CRP levels.

## MATERIALS AND METHODS

### Eligibility

The Institutional Review Board of our institute approved this retrospective study, and the need for written informed consent was waived. Patient records/information was anonymized and deidentified before analysis. Using our prospectively collected CRC database, we selected patients who underwent both  $^{18}\text{F}$ -FDG PET/CT scan, before surgery, and KRAS mutation examination, between August 2006 and April 2014. Patients were excluded from the selection if they were diagnosed with hereditary nonpolyposis CRC or synchronous cancer, had undergone preoperative chemotherapy or radiotherapy, and had no CRP level results before the PET/CT scan was undertaken. Clinicopathologic information on sex; age; body mass index; history of diabetes mellitus; histologic grade; lymphovascular invasion; carcinoembryonic antigen; tumor size; location of the primary tumor in the proximal colon (cecal, ascending, and transverse colon), distal colon (descending, sigmoid, and rectosigmoid colon), or rectum; and pathologic T and N stages were extracted from our database. Among the 221 patients who underwent  $^{18}\text{F}$ -FDG PET/CT scan and KRAS mutation analysis for CRC during the study period, 179 with full clinicopathologic information were included in this study (Fig. 1).

### $^{18}\text{F}$ -FDS Positron Emission Tomography/Computed Tomography Protocol

All patients fasted for at least 6 hours and had blood glucose levels less than 140 mg/dL before intravenous administration of  $^{18}\text{F}$ -FDG (5.5 MBq/kg of body weight). At 60 minutes after intravenous administration of  $^{18}\text{F}$ -FDG, PET/CT scans were performed with a hybrid PET/CT scanner (Biograph 40 TruePoint or Biograph mCT 64, Siemens Healthcare Solutions USA, Inc.,

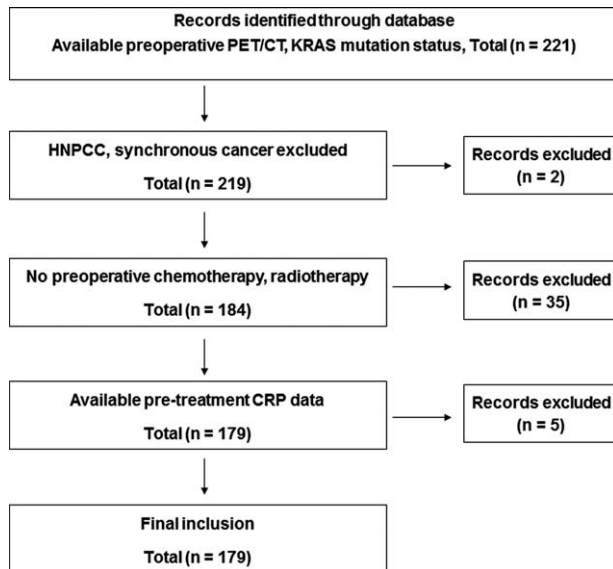


FIGURE 1. Exclusion criteria and patient selection diagram.

Knoxville, TN). Whole-body CT images were obtained first for attenuation correction using automatic dose modulation with a reference of 40 mA and 120 kV without contrast enhancement. Then PET data were acquired from the skull base to the proximal thigh for 3 minutes per bed position in a three-dimensional mode. Positron emission tomography images were reconstructed with the ordered subset expectation maximization algorithm.

### Image Analysis

$^{18}\text{F}$ -FDG PET/CT images were reviewed in consensus from 2 experienced nuclear medicine physicians who were blinded to clinicopathologic results at the time of the review. The maximum standardized uptake value ( $\text{SUV}_{\text{max}}$ ) was calculated as follows:  $\text{SUV}_{\text{max}} = C_{\text{max}} \times \text{TBW}/\text{IA}$  [ $C_{\text{max}}$ : activity concentration in the voxel of highest tumor activity (Bq/mL), TBW: total body weight (kg), IA: injected activity (kBq)]. The peak SUV ( $\text{SUV}_{\text{peak}}$ ) was calculated as the average SUV within a 1.2-cm diameter spherical volume of interest (VOI) positioned around the voxel of the highest SUV.

The metabolic tumor volume (MTV) was measured using a SUV-based automated contouring program (Syngo.via, version VA20A, Siemens Medical Solutions, Erlangen, Germany). First, a VOI was drawn large enough to incorporate the primary tumor lesion in the axial, coronal, and sagittal  $^{18}\text{F}$ -FDG PET/CT images. For the determination of metabolic volumes, we used 50% of  $\text{SUV}_{\text{max}}$  as a threshold, as 50%  $\text{SUV}_{\text{max}}$  threshold was shown to best fit the actual volume of simulating phantom lesions in previous studies.<sup>12</sup> The software automatically produced the contour around the target lesion inside the VOI and the voxels presenting SUV intensity higher than the threshold within the contouring margin were incorporated to define the tumor volume. Total lesion glycolysis (TLG) was calculated by multiplying the tumor volume by the mean SUV of the volume.

### V-Ki-Ras2 Kirsten Rat Sarcoma Viral Oncogene Homolog Mutation Status Evaluation

Deoxyribonucleic acid was extracted from formalin-fixed, paraffin-embedded tumor tissue slides with the MagNA Pure 96 System (Roche Applied Science, Indianapolis, IN). V-Ki-ras2

Kirsten rat sarcoma viral oncogene homolog exon 2 was amplified by polymerase chain reaction using GeneAMP PCR system veriti (Applied Biosystems, Foster City, CA), and was analyzed using direct sequencing with the Applied Biosystems 3730XL automated DNA analyzer (Applied Biosystems, Foster City, CA) according to the manufacturer's instruction. The sequences of the primer were as follows: forward, GGAATTTTCATGATT-GAATTTTGT; reverse, GAACATCATGGACCCTGACA.

## Statistical Analysis

Our study group was divided into 2 subgroups (the normal CRP group and the elevated CRP group) according to levels of CRP before the PET/CT scan. All enrolled patients had CRP data obtained within 2 days of the PET/CT scan. The differences in clinicopathologic features and PET/CT parameters between the KRAS wild-type group and the KRAS mutated group were analyzed using 2-sided Pearson  $\chi^2$  test or Fisher exact test for categorical variables and with a Student *t* test for continuous variables. Then, the cutoff values of the variables providing the best separation between the KRAS wild-type and mutated groups were obtained using receiver operating characteristic curve analyses, and used to dichotomize the data. Predictive values of PET/CT parameters for the KRAS status were evaluated using multivariate logistic regression analysis along with the clinicopathologic variables. Multicollinearity among PET/CT-related parameters was evaluated by calculating Spearman rank correlation coefficient before multivariate analysis. To evaluate the impact of CRP status on predictive values of PET/CT-related parameters for KRAS mutation, the same statistical analyses were performed after the patients were divided into the 2 groups: the normal CRP group and the elevated CRP group. A *P* value <0.05 was considered to indicate statistical significance. All calculations and analysis were performed using the SPSS software package Version 20.0 (IBM Corp., Armonk, NY).

## RESULTS

### Patient Demographics

The characteristics of the 179 enrolled patients are shown in Table 1. We evaluated the differences in clinicopathologic variables and PET/CT-related parameters according to CRP levels with a cutoff level of 6.0 mg/L. The patients with elevated CRP levels (*n* = 47; 26.2%) had primary tumors of larger size and higher SUV<sub>max</sub>, SUV<sub>peak</sub>, MTV, and TLG, compared with those with normal CRP levels (*n* = 132; 73.8%; *P* < 0.05, all). V-Ki-ras2 Kirsten rat sarcoma viral oncogene homolog mutations were found in 60 patients (33.5%); 45 of these patients (75%) had normal CRP levels, whereas the other 15 patients (25%) showed elevated CRP levels. On review of medical records, none of the patients with abnormal CRP levels had any severe systemic inflammation or infection that might have contributed to elevations in CRP level. The other clinicopathologic factors did not show significant group differences.

### Factors Associated With V-Ki-Ras2 Kirsten Rat Sarcoma Viral Oncogene Homolog Mutation Status

A cutoff level was determined by receiver operating characteristic curve analysis for SUV<sub>max</sub>, SUV<sub>peak</sub>, MTV, and TLG, and the best discriminative values between those tumors with wild-type and mutated KRAS were 10 (g/mL), 7.4 (g/mL), 10 mL, and 50 g, respectively. Among the 179 patients

in total, the KRAS mutation group was found to have tumors with lower histologic grade and more positive lymph node (LN) metastasis, compared with the KRAS wild-type group (*P* < 0.05, all; Table 2). None of the PET/CT-related parameters showed significant differences between the 2 groups. Multivariate analysis revealed that histologic grade and LN metastasis were independent predictors of KRAS mutation in CRC patients [histologic grade: odds ratio (OR), 5.6; 95% confidence interval (CI), 1.6–18.9; *P* = 0.006, and LN metastasis: OR, 3.4; 95% CI, 1.6–7.1; *P* = 0.001].

### Subgroup Analysis According to C-Reactive Protein Level

In the normal CRP group (CRP < 6; *n* = 132), the KRAS mutation group showed higher SUV<sub>max</sub>, SUV<sub>peak</sub>, and lower histologic grade than the KRAS wild-type group. In the prediction of KRAS mutation, the sensitivity, specificity, and accuracy were 60.0%, 50.3%, and 54.0% for SUV<sub>max</sub> and 73.3%, 60.5%, and 67.8% for SUV<sub>peak</sub>, respectively. Because a strong positive correlation was found between SUV<sub>max</sub> and SUV<sub>peak</sub> (Spearman rho = 0.955, *P* < 0.01), their predictive values were analyzed in 2 separate multivariate models. In multivariate logistic regression analysis, higher SUV<sub>max</sub> proved to be significantly associated with KRAS mutation together with lower histologic grade and positive LN metastasis (SUV<sub>max</sub>: OR, 3.3; 95% CI, 1.4–7.4; *P* = 0.005, histologic grade: OR, 6.0; 95% CI, 1.5–24.6; *P* = 0.013, positive LN metastasis: OR, 3.2; 95% CI, 1.3–7.8; *P* = 0.011; Table 3). In the model with SUV<sub>peak</sub>, SUV<sub>peak</sub> was also found to be an independent predictor of KRAS mutation, along with histologic grade and LN metastasis (SUV<sub>peak</sub>: OR, 3.8; 95% CI, 1.5–9.3; *P* = 0.004, histologic grade: OR, 5.5; 95% CI, 1.3–22.8; *P* = 0.019, positive LN metastasis: OR, 3.1; 95% CI, 1.9–7.5; *P* = 0.015). In contrast, both lower <sup>18</sup>F-FDG uptake and positive LN metastasis were significantly associated with KRAS mutation in the elevated CRP group (CRP ≥ 6; *n* = 47; *P* < 0.05, all).

## DISCUSSION

V-Ki-ras2 Kirsten rat sarcoma viral oncogene homolog mutational analysis is essential before the initiation of anti-EGFR therapy, because the antitumor efficacy of the drug is dependent on KRAS mutation status. The most common methods of assessing KRAS mutational status are through molecular examination using biopsy or resected tissue. There, however, there are several obstacles to this approach. First, in case of metastatic sites, it is not always easy to access or obtain adequate tissue samples for genetic testing. Second, because of the nonhomogeneous, scattered distribution of tumor tissue, there could be discordant results for KRAS mutation between the biopsy tissue and the resected tumor.<sup>13,14</sup> For these reasons, Miles et al<sup>15</sup> insisted that identification of an imaging signature for the KRAS mutation would enable imaging to provide an adjunct to histologic assessment, and demonstrated that decision trees using imaging biomarkers could enhance the predictive accuracy of KRAS mutation in CRC.

<sup>18</sup>F-FDG PET/CT is now being widely used in staging, detecting recurrence, monitoring treatment response, and predicting prognosis in CRC; however, <sup>18</sup>F-FDG PET/CT has been used relatively rarely in the investigation of gene expression. Only a few studies have evaluated the association between <sup>18</sup>F-FDG uptake and KRAS mutation. Kawada et al<sup>6</sup> reported that the SUV<sub>max</sub> and the tumor-to-liver ratio were significantly higher in the group of patients with KRAS mutation. Another

**TABLE 1.** Patient Characteristics According to C-Reactive Protein Status (n = 179)

Variables	Total (n = 179)	CRP < 6 (n = 132)	CRP ≥ 6 (n = 47)	P
Sex				0.603
Male:female	101:78	76:56	25:22	
Age (years)				0.850
Mean ± SD	64.0 ± 1.2	63.9 ± 12.0	64.3 ± 13.0	
BMI (kg/m <sup>2</sup> )				0.583
Mean ± SD	23.1 ± 3.2	23.2 ± 3.1	22.9 ± 3.5	
DM				0.858
Yes	32	24	8	
No	147	108	39	
CEA (ng/mL)				0.202
Mean ± SD	10.4 ± 31.2	7.6 ± 16.3	18.2 ± 54.6	
Tumor location				0.080
Proximal colon	60	38	22	
Distal colon	63	80	13	
Rectum	56	44	12	
Tumor size (cm)				<0.001
Mean ± SD	5.1 ± 3.4	4.5 ± 2.4	6.2 ± 2.6	
Histologic grade*				0.362
G1	14	12	2	
G2, G3, etc.	165	120	45	
LVI				0.666
Positive	49	35	14	
Negative	130	97	33	
pT				0.191
Tis, T1, and T2	30	25	5	
T3 and T4	149	107	42	
LN metastasis				0.630
Positive	93	70	23	
Negative	86	62	24	
Stage				0.891
0 and I	24	19	5	
II	58	41	17	
III	79	59	20	
IV	18	13	5	
SUV <sub>max</sub>				0.029
Mean ± SD	12.0 ± 6.3	11.4 ± 6.2	13.7 ± 6.2	
SUV <sub>peak</sub>				0.025
Mean ± SD	9.8 ± 5.2	9.2 ± 5.0	11.2 ± 5.3	
MTV				0.002
Mean ± SD	20.2 ± 22.3	15.7 ± 12.7	32.8 ± 35.2	
TLG				<0.001
Mean ± SD	145.4 ± 169.4	105.1 ± 98.5	258.3 ± 256.3	

BMI = body mass index, CEA = carcinoembryonic antigen, CRP = C-reactive protein, DM = diabetes mellitus, LN = lymph node, LVI = lymphovascular invasion, MTV = metabolic tumor volume, SD = standard deviation, SUV<sub>max</sub> = maximum standardized uptake value, SUV<sub>peak</sub> = peak standardized uptake value, TLG = total lesion glycolysis.

\* Union for International Cancer Control (UICC) classification: G1 well differentiated, G2 moderately differentiated, G3 poorly differentiated, etc. mucinous and signet ring cell.

retrospective study also showed that SUV<sub>max</sub> was an independent predictor of KRAS mutation in CRC, together with the PET-based maximal tumor width.<sup>5</sup> The accuracy of SUV<sub>max</sub> improved when combined with other imaging features: SUV<sub>max</sub>, CT texture, and perfusion.<sup>15</sup> Recently, Iwamoto et al<sup>7</sup> suggested that mutated KRAS causes higher <sup>18</sup>F-FDG accumulation, possibly by upregulation of GLUT1, through an in vitro study. In contrast, a recent clinical study reported a lack of association between KRAS mutation and <sup>18</sup>F-FDG uptake in metastatic colon cancer.<sup>8</sup> This study also showed that there was

no significant association between GLUT1 mRNA expression and KRAS mutation status.

Based on our results, we suppose that the lack of association between KRAS mutation and <sup>18</sup>F-FDG uptake, however, might be because of improper patient selection. In the other clinical studies, patients with high serum glucose levels, small-sized tumors, or high CPR levels of >5 mg/L were excluded on the rationale that those variables might interfere with <sup>18</sup>F-FDG uptake and accurate measurement of SUV.<sup>5,6</sup> In the current study, <sup>18</sup>F-FDG uptake represented as SUV<sub>max</sub> and SUV<sub>peak</sub> had

**TABLE 2.** Univariate Analysis of Factors Associated With V-Ki-Ras2 Kirsten Rat Sarcoma Viral Oncogene Homolog Status According to C-Reactive Protein Level

Variables	Total		CRP < 6		P	CRP ≥ 6		p
	Wild-Type KRAS (n = 119)	Mutated KRAS (n = 60)	Wild-Type KRAS (n = 87)	Mutated KRAS (n = 45)		Wild-type KRAS (n = 32)	Mutated KRAS (n = 15)	
Sex								
Male	71	30	53	23	0.280	18	7	0.539
Female	48	30	34	22		14	8	
Age (years)								
<60	41	18	30	13	0.516	11	5	0.944
≥60	78	42	57	32		21	10	
BMI (kg/m <sup>2</sup> )								
<25	87	44	64	35	0.596	23	9	0.327
≥25	31	16	23	10		8	6	
DM history								
Yes	24	8	17	7	0.596	7	1	0.327
No	95	52	70	38		25	14	
CEA (ng/mL)								
<5	76	36	58	29	0.065	18	7	0.377
≥5	43	24	29	16		14	8	
Tumor location								
Proximal	38	22	25	13	0.420	13	9	0.348
Distal	45	18	36	14		9	4	
Rectum	36	20	26	18		10	2	
Tumor size (cm)								
<5	60	31	51	28	0.689	9	3	0.552
≥5	59	29	36	17		23	12	
Histologic grade*								
G1	5	9	4	8	0.013	1	1	0.575
G2, G3, etc.	114	51	83	37		31	14	
LVI								
Positive	35	14	26	9	0.223	9	5	0.716
Negative	48	46	61	36		23	10	
pT								
Tis, T1, T2	20	10	15	10	0.489	5	0	0.105
T3, T4	99	50	72	35		27	15	
LN metastasis								
Positive	54	39	42	28	0.128	12	11	0.022
Negative	65	21	45	17		20	4	
Stage								
0 and I	18	6	13	6	0.547	5	0	0.017
II	43	15	30	11		13	4	
III	46	33	37	22		9	11	
IV	12	6	7	6		5	0	
Maximum Standardized Uptake Value								
Mean ± SD	11.8 ± 5.7	12.6 ± 7.4	10.4 ± 4.6	13.2 ± 8.1	0.037	15.3 ± 6.5	10.4 ± 4.1	0.012
≥10	63	38	39	32	0.004	24	6	0.020
<10	56	22	48	13		8	9	
Peak Standardized Uptake Value								
Mean ± SD	9.7 ± 4.8	10.0 ± 5.9	8.5 ± 3.9	10.6 ± 6.5	0.022	12.6 ± 5.6	8.2 ± 2.9	0.001
≥7.4	72	45	48	37	0.002	24	8	0.137
<7.4	47	15	39	8		8	7	
Metabolic Tumor Volume (mL)								
Mean ± SD	21.1 ± 25.9	18.5 ± 12.5	16.2 ± 14.5	14.8 ± 8.1	0.556	34.4 ± 41.2	29.3 ± 16.7	0.647
≥13	60	38	38	25	0.195	22	13	0.189
<13	59	22	49	20		10	2	
Total Lesion Glycolysis (g)								
Mean ± SD	153.7 ± 196.9	128.9 ± 93.0	101.6 ± 106.8	112.0 ± 80.8	0.568	295.2 ± 295.8	179.6 ± 110.7	0.059
≥50	86	49	58	36	0.109	28	13	0.936
<50	33	11	29	9		4	2	

BMI = body mass index, CEA = carcinoembryonic antigen, CRP = C-reactive protein, DM = diabetes mellitus, KRAS = v-Ki-ras2 Kirsten rat sarcoma viral oncogene homolog, LN = lymph node, LVI = lymphovascular invasion, SD = standard deviation.

\* Union for International Cancer Control (UICC) classification: G1 well differentiated, G2 moderately differentiated, G3 poorly differentiated, etc. mucinous and signet ring cell.

a positive correlation with KRAS mutation only in the normal CRP group; meanwhile, it showed an inverse correlation in the elevated CRP group and lost its predictive power in the whole population. <sup>18</sup>F-FDG is a glucose analogue and thus a metabolic tracer, not a cancer-specific tracer. Secondary local

inflammation following treatment has been shown to induce false-positive <sup>18</sup>F-FDG accumulation, thus hampering the acute assessment of treatment response. Kubota et al<sup>10</sup> demonstrated that newly formed granulation tissue around tumors and macrophages showed greater FDG uptake than did viable tumor cells,

**TABLE 3.** Multivariate Analysis and Estimation of Odds Ratios for Predicting V-Ki-Ras2 Kirsten Rat Sarcoma Viral Oncogene Homolog Mutation in Patients With Normal C-Reactive Protein Level (n = 132)

		Model With SUV <sub>max</sub>		Model With SUV <sub>peak</sub>	
		OR (95% CI)	P	OR (95% CI)	P
Histologic grade*	G1 versus G2/G3/etc.	6.0 (1.5–24.6)	0.013	5.5 (1.3–22.8)	0.019
LVI	Positive	0.5 (0.2–1.2)	0.125	0.5 (0.2–1.2)	0.125
LN metastasis	Positive	3.2 (1.3–7.8)	0.011	3.1 (1.3–7.5)	0.014
SUV <sub>max</sub>	≥10 versus <10	3.3 (1.4–7.4)	0.005		
SUV <sub>peak</sub>	≥7.4 versus <7.4			3.8 (1.5–9.3)	0.004

CI = confidence interval, LN = lymph node, LVI = lymphovascular invasion, OR = odds ratio, SUV<sub>max</sub> = maximum standardized uptake value, SUV<sub>peak</sub> = peak standardized uptake value.

\* Union for International Cancer Control (UICC) classification: G1 well differentiated, G2 moderately differentiated, G3 poorly differentiated, etc. mucinous and signet ring cell.

and a maximum of 29% of the <sup>18</sup>F-FDG uptake was derived from nontumor tissues, such as macrophages and granulation tissues, which was indicative of confusing <sup>18</sup>F-FDG uptake in the inflammatory response to tumor cells. Diederichs et al<sup>11</sup> evaluated the accuracy of FDG-PET concerning the differentiation of benign and malignant pancreatic masses according to CRP level. In the differentiation of benign and malignant lesions, specificity was significantly lower for patients with elevated CRP levels than for patients with unknown or normal CRP levels (40% versus 87%,  $P < 0.01$ ). They concluded that elevated CRP may cause false-positive results in FDG-PET examinations. Nevertheless, to the best of our knowledge, the relationships among CRP level, local inflammation, and tumoral <sup>18</sup>F-FDG uptake in CRC have not been investigated thoroughly.

Causes of local inflammation in CRC can be postulated in 2 aspects: 1 is from host-to-tumor response and the other from gross peritumoral tissue damage. Solid tumors comprise malignant cells, resident stromal cells, and infiltrating inflammatory leukocytes.<sup>16</sup> Peritumoral inflammatory lesions are extensively infiltrated by activated macrophages, so-called tumor-associated macrophages.<sup>17,18</sup> Besides the host response, CRC may be accompanied by tumor necrosis, perforation, abscess formation, or bowel ischemia that predisposes it to inflammatory cell infiltration. A high-degree local inflammatory cell response is reportedly more commonly present in rectal tumors,<sup>19</sup> whereas an elevated systemic inflammatory response is more commonly present in colonic tumors.<sup>20</sup> Those phagocytes are also effective accumulators of <sup>18</sup>F-FDG because of their constitutively high endocytic activity,<sup>10</sup> and thus, accumulation of inflammatory cells is often associated with false-positive results in <sup>18</sup>F-FDG-based studies.<sup>21–23</sup> Admittedly, CRP is an acute-phase marker for systemic inflammation and therefore may be not directly related to local inflammatory response. A high-grade local inflammatory response, however, can switch to a systemic inflammatory response as tumor growth continues or inflammation is aggravated.<sup>24</sup> For those reasons, abnormal elevation of CRP may suggest the presence of local inflammation in CRC, and accurate quantification of <sup>18</sup>F-FDG uptake in CRC could be hampered in this condition. The current study reinforces the importance of proper patient selection that has been highlighted in other studies.<sup>11</sup>

<sup>18</sup>F-FDG PET/CT has several advantages over other potential biologic or imaging markers in prediction of KRAS mutation. This technique is a noninvasive functional imaging modality that provides quantitative information on the glucose uptake of tumors as well as qualitative features of tumors that may provide guidance on

decisions regarding biopsy sites. In addition, the metabolic parameters of the primary lesion can be obtained before or without surgery. Moreover, contouring of the tumor and measurement of SUV<sub>max</sub> are less operator dependent and there is less interobserver variability, compared with conventional imaging modalities.<sup>25–27</sup> Nevertheless, for prediction of KRAS mutation in CRC, the overall accuracy of SUV<sub>max</sub> alone has only been found to be modest, ranging from 60% to 75%, and this was similar in our study. Although the accuracy could be improved when combined with other clinicopathologic or imaging parameters, <sup>18</sup>F-FDG PET/CT cannot replace conventional methods to confirm KRAS mutation, and it should rather be used as a complementary tool when histopathologic results are equivocal.

There are several limitations in this study. First, CRP is related to local inflammation, although probably indirectly. Therefore, peritumoral inflammation does affect the measurement of SUV in primary tumors; however, this study lacks histopathologic confirmation of secondary local inflammation and it is unclear how accurately CRP level reflects the severity of such local inflammation. Second, we used 0 to 6 mg/L as the normal range of CRP levels. These values, however, may be less generalizable because reference CRP values vary from laboratory to laboratory, as does the definition of severe inflammation in terms of CRP. Lastly, despite a larger population of CRC patients, this was a retrospective study conducted at a single tertiary referral center.

In conclusion, <sup>18</sup>F-FDG uptake in primary CRCs with mutated KRAS was significantly higher than in CRCs with wild-type KRAS, and SUV<sub>max</sub> and SUV<sub>peak</sub> were independent predictors of KRAS mutation together with positive LN metastasis. This relationship, however, changed in patients with elevated CRP levels, and we suppose that severe local inflammation might have affected the measurement of tumoral <sup>18</sup>F-FDG uptake. The current study reinforced the predictive value of <sup>18</sup>F-FDG uptake for KRAS mutation in addition to stressing the importance of proper patient selection in a correlative study.

## REFERENCES

1. Van Cutsem E, Kohne CH, Hitre E, et al. Cetuximab and chemotherapy as initial treatment for metastatic colorectal cancer. *N Engl J Med*. 2009;360:1408–1417.
2. Schrag D. The price tag on progress: chemotherapy for colorectal cancer. *N Engl J Med*. 2004;351:317–319.
3. Ren J, Li G, Ge J, et al. Is K-ras gene mutation a prognostic factor for colorectal cancer: a systematic review and meta-analysis. *Dis Colon Rectum*. 2012;55:913–923.

4. Park J, Chang K, Seo Y, et al. Tumor SUVmax normalized to liver uptake on 18F-FDG PET/CT predicts the pathologic complete response after neoadjuvant chemoradiotherapy in locally advanced rectal cancer. *Nucl Med Mol Imaging*. 2014;48:295–302.
5. Chen SW, Chiang HC, Chen WT, et al. Correlation between PET/CT parameters and KRAS expression in colorectal cancer. *Clin Nucl Med*. 2014;39:685–689.
6. Kawada K, Nakamoto Y, Kawada M, et al. Relationship between 18F-fluorodeoxyglucose accumulation and KRAS/BRAF mutations in colorectal cancer. *Clin Cancer Res*. 2012;18:1696–1703.
7. Iwamoto M, Kawada K, Nakamoto Y, et al. Regulation of 18F-FDG accumulation in colorectal cancer cells with mutated KRAS. *J Nucl Med*. 2014;55:2038–2044.
8. Krikelis D, Skoura E, Kotoula V, et al. Lack of association between KRAS mutations and 18F-FDG PET/CT in Caucasian metastatic colorectal cancer patients. *Anticancer Res*. 2014;34:2571–2579.
9. Kubota K. From tumor biology to clinical Pet: a review of positron emission tomography (PET) in oncology. *Ann Nucl Med*. 2001;15:471–486.
10. Kubota R, Yamada S, Kubota K, et al. Intratumoral distribution of fluorine-18-fluorodeoxyglucose in vivo: high accumulation in macrophages and granulation tissues studied by microautoradiography. *J Nucl Med*. 1992;33:1972–1980.
11. Diederichs CG, Staib L, Glasbrenner B, et al. F-18 fluorodeoxyglucose (FDG) and C-reactive protein (CRP). *Clin Positron Imaging*. 1999;2:131–136.
12. Uto F, Shiba E, Onoue S, et al. Phantom study on radiotherapy planning using PET/CT: delineation of GTV by evaluating SUV. *J Radiat Res*. 2010;51:157–164.
13. Krol LC, Hart NA, Methorst N, et al. Concordance in KRAS and BRAF mutations in endoscopic biopsy samples and resection specimens of colorectal adenocarcinoma. *Eur J Cancer*. 2012;48:1108–1115.
14. Pang NK, Nga ME, Chin SY, et al. KRAS and BRAF mutation analysis can be reliably performed on aspirated cytological specimens of metastatic colorectal carcinoma. *Cytopathology*. 2011;22:358–364.
15. Miles KA, Ganeshan B, Rodriguez-Justo M, et al. Multifunctional imaging signature for V-KI-RAS2 Kirsten rat sarcoma viral oncogene homolog (KRAS) mutations in colorectal cancer. *J Nucl Med*. 2014;55:386–391.
16. Cottone L, Valtorta S, Capobianco A, et al. Evaluation of the role of tumor-associated macrophages in an experimental model of peritoneal carcinomatosis using (18)F-FDG PET. *J Nucl Med*. 2011;52:1770–1777.
17. Bacci M, Capobianco A, Monno A, et al. Macrophages are alternatively activated in patients with endometriosis and required for growth and vascularization of lesions in a mouse model of disease. *Am J Pathol*. 2009;175:547–556.
18. Kawamura K, Komohara Y, Takaishi K, et al. Detection of M2 macrophages and colony-stimulating factor 1 expression in serous and mucinous ovarian epithelial tumors. *Pathol Int*. 2009;59:300–305.
19. Klintrup K, Makinen JM, Kauppila S, et al. Inflammation and prognosis in colorectal cancer. *Eur J Cancer*. 2005;41:2645–2654.
20. McMillan DC, Crozier JE, Canna K, et al. Evaluation of an inflammation-based prognostic score (GPS) in patients undergoing resection for colon and rectal cancer. *Int J Colorectal Dis*. 2007;22:881–886.
21. Brewer S, McPherson M, Fujiwara D, et al. Molecular imaging of murine intestinal inflammation with 2-deoxy-2-[18F]fluoro-D-glucose and positron emission tomography. *Gastroenterology*. 2008;135:744–755.
22. Rosenbaum SJ, Lind T, Antoch G, et al. False-positive FDG PET uptake: the role of PET/CT. *Eur Radiol*. 2006;16:1054–1065.
23. Yamada S, Kubota K, Kubota R, et al. High accumulation of fluorine-18-fluorodeoxyglucose in turpentine-induced inflammatory tissue. *J Nucl Med*. 1995;36:1301–1306.
24. Roxburgh CS, Salmond JM, Horgan PG, et al. The relationship between the local and systemic inflammatory responses and survival in patients undergoing curative surgery for colon and rectal cancers. *J Gastrointest Surg*. 2009;13:2011–2018.
25. Lambrecht M, Haustermans K. Clinical evidence on PET-CT for radiation therapy planning in gastro-intestinal tumors. *Radiother Oncol*. 2010;96:339–346.
26. Lee JA. Segmentation of positron emission tomography images: some recommendations for target delineation in radiation oncology. *Radiother Oncol*. 2010;96:302–307.
27. Patel DA, Chang ST, Goodman KA, et al. Impact of integrated PET/CT on variability of target volume delineation in rectal cancer. *Technol Cancer Res Treat*. 2007;6:31–36.